

## World sheet formulation for lattice staggered fermions

J. M. Aroca

*Departament de Matemàtiques, Universitat Politècnica de Catalunya, Jordi Girona 1-3, Mod C-3 Campus Nord, 08034 Barcelona, Spain*

Hugo Fort and Rodolfo Gambini

*Instituto de Física, Facultad de Ciencias, Tristan Narvaja 1674, 11200 Montevideo, Uruguay*

(Received 12 September 1997; published 2 February 1998)

The world sheet formulation is introduced for lattice gauge theories with dynamical fermions. The partition function of lattice compact QED with staggered fermions is expressed as a sum over surfaces with a border on self-avoiding fermionic paths. The surfaces correspond to the world sheets of loop-like pure electric flux excitations and meson-like configurations (open electric flux tubes carrying matter fields at their ends). The proposed formulation does not have the problem of the additional doubling of the fermion species due to the discretization of time. The gauge non-redundancy and the geometric transparency are two appealing features of this description. From the computational point of view, the partition function involves fewer degrees of freedom than the Kogut-Susskind formulation and offers an alternative and more economic framework to perform numerical computations with dynamical fermions. [S0556-2821(98)00106-4]

PACS number(s): 11.15.Ha

### I. INTRODUCTION

The problem of handling dynamical fermions is still a major challenge that faces lattice gauge theory at present. Monte Carlo techniques have provided many important results clarifying several points about the dynamic, and recent computations are achieving 10% or better accuracy in the spectrum both for heavy quark and light quark system [1]. However, statistical algorithms are very expensive in computer time, and the increased computing power of the coming generation of machines without further theoretical insight will probably be insufficient in order to definitely improve results. Basically, the difficulty posed by the fermions stems from the fact that they are represented not by ordinary numbers but by anti-commuting Grassmann numbers which cannot be directly simulated numerically. Since the fermion field appears quadratically in the action, the usual procedure is to integrate it out producing the Matthews-Salam determinant. So, the problem of including dynamical fermions is reduced to one of evaluating the determinant of a large matrix. This is a costly task.

An alternative to tackle this problem is to resort to the analytical methods. These could be divided into two categories: strong-coupling expansion and Hamiltonian variational-like methods. The principal limitation of the former is the difficulty to reach the weak-coupling region. An exponent of the second group is the *loop* approach [2,3]. The basis of the loop method can be traced to the idea of describing gauge theories explicitly in terms of Wilson loops or holonomies [4,5] since Yang [6] noticed their important role for a complete description of gauge theories. The loop Hamiltonian was given in terms of two fundamental operators: the Wilson Loop operator (the trace of the holonomy) and the electric field operator (its temporal loop derivative). The loops replace the information furnished by the vector potential (the connection). A description in terms of loops or strings, in addition to the general advantage of only involving the gauge invariant physical excitations, is appealing because all the

gauge invariant operators have a simple geometrical meaning when realized in the loop space. Last but not least, the interest on loops relies on the fact that it was realized that this formalism goes beyond a simple gauge invariant description and in fact it provides a natural geometrical framework to treat gauge theories and quantum gravity. The introduction by Ashtekar [7] of a new set of variables that cast general relativity in the same language as gauge theories allowed one to apply loop techniques as a natural non-perturbative description of Einstein's theory.

In 1991 the *loop* representation was extended in such a way to include dynamical staggered [8] fermions: the so-called *P-representation* [9]. Roughly the idea is to add to the closed pure gauge excitations, open ones corresponding to "electromesons." Afterwards the P-representation was used to perform analytical Hamiltonian calculations, by means of a cluster approximation, providing qualitatively good results for the (2+1) [10] and the (3+1) [11] cases when compared with the standard Lagrangian numerical simulations in terms of the fields. The Hamiltonian method has the serious drawback of the explosive proliferation of clusters with the order of the approximation.

Thus, our goal was to explore another approach: to build a classical action in terms of strings and knit together the transparency and non-redundance of the string P-formulation and the power of the Lagrangian simulations. The first step of this program was the introduction of new lattice action for pure QED in terms of closed strings of electric flux (loops) [12]. In the pure case the action is written as a sum of integer variables attached to the closed world sheets of the loop excitations. The second step was to include matter fields into the string description; with this aim we considered the simplest gauge theory: the compact scalar electrodynamics (SQED) [13]. In the case of SQED the action is expressed in terms of open and closed surfaces which correspond to world sheets of loop-like pure electric flux excitations and open electric flux tubes carrying matter fields at their ends. The previous two world sheets actions were simulated using the

Metropolis algorithm, the results being quite encouraging [12,13].

Here we show how to introduce dynamical fermions in a world sheet or Lagrangian description. This paper is organized as follows. Section II is a ‘‘bird’s-eye-view’’ review of the P-representation on a hypercubic lattice. We show the realization of the lattice QED Hamiltonian in the Hilbert space of paths  $\{P\}$ . In Sec. III we present the Lagrangian counterpart of the previous P-representation and we write the partition function in terms of world sheets of the string-like excitations. In Sec. IV, by using the transfer matrix procedure, we check that we get the Hamiltonian of Sec. II from the path integral of Sec. III. Notice that this enabled us to get the Kogut-Susskind formulation via the transfer matrix; this is an interesting problem which was not properly solved. Finally, Sec. V is devoted to conclusions and some remarks.

## II. THE P-REPRESENTATION ON THE LATTICE

The P-representation offers a gauge invariant description of physical states in terms of kets  $|P\rangle$ , where  $P$  labels a set of connected paths  $P_x^y$  with ends  $x$  and  $y$ .<sup>1</sup> In order to make the connection on the lattice between the P-representation and the ordinary representation, in terms of the fermion fields  $\psi$  and the gauge fields  $U_\mu(x) = \exp[ieaA_\mu(x)]$ , we need a gauge invariant object constructed from them. The most natural candidate in the continuum is

$$\Phi(P_x^y) = \psi^\dagger(x)U(P_x^y)\psi(y), \quad (1)$$

where  $U(P_x^y) = \exp[iea \int_P A_\mu dx^\mu]$ .

The immediate problem we face is that  $\Phi$  is not purely an object belonging to the ‘‘configuration’’ basis because it includes the canonical conjugate momentum of  $\psi$ ,  $\psi^\dagger$ . The lattice offers a solution to this problem consisting in the decomposition of the fermionic degrees of freedom. Let us consider the Hilbert space of kets  $|\psi_u^\dagger, \psi_d, A_\mu\rangle$ , where  $u$  corresponds to the *up* part of the Dirac spinor and  $d$  to the *down* part. Those kets are well defined in terms of ‘‘configuration’’ variables (the canonical conjugate momenta of  $\psi_d$  and  $\psi_u^\dagger$  are  $\psi_d^\dagger$  and  $\psi_u$  respectively). Then, the internal product of one of such kets with one of the path dependent representation (characterized by a lattice path  $P_x^y$  with ends  $x$  and  $y$ ) is given by

$$\Phi(P_x^y) \equiv \langle P_{x;i}^{y;j} | \psi_u^\dagger, \psi_d, A_\mu \rangle = \psi_{u;i}^\dagger(x)U(P_x^y)\psi_{d;j}(y), \quad (2)$$

where  $i$  and  $j$  denote a component of the spinor  $u$  and  $d$  respectively. Thus, it seems that the choice of staggered fermions is the natural one in order to build the lattice P-representation. Therefore, the lattice paths  $P_x^y$  start in sites  $x$  of a given parity and end in sites  $y$  with opposite parity. The one spinor component at each site can be described in terms

of the  $\chi(x)$  single Grassmann fields [8]. The path creation operator  $\hat{\Phi}_Q$  in the space of kets  $\{|P\rangle\}$  of a path with ends  $x$  and  $y$  is defined as

$$\hat{\Phi}_Q = \hat{\chi}^\dagger(x)\hat{U}(Q_x^y)\hat{\chi}(y). \quad (3)$$

Its adjoint operator  $\hat{\Phi}_Q^\dagger$  acts in two possible ways [9]: annihilating the path  $Q_x^y$  or joining two existing paths in  $|P\rangle$ , one ending at  $x$  and the other starting at  $y$ .

Let us show the realization of the QED Hamiltonian in the Hilbert space of kets  $|P\rangle$ . This Hamiltonian is given by

$$\hat{H} = (g^2/2)\hat{W}$$

$$\hat{W} = \hat{W}_E + \lambda \hat{W}_I + \lambda^2 \hat{W}_M$$

$$\lambda = 1/g^2$$

$$\hat{W}_E = \sum_{\ell} \hat{E}_{\ell}^2$$

$$\hat{W}_I = - \sum_{\ell} (\hat{\Phi}_{\ell} + \hat{\Phi}_{\ell}^\dagger) \quad (4)$$

$$(\hat{\Phi}_{\ell}^\dagger = \eta_n(x)\hat{\chi}^\dagger(x)\hat{U}_n(x)\hat{\chi}(x+n))$$

$$\eta_{\mathbf{e}_i}(x) = (-1)^{x_1 + \dots + x_{i-1}},$$

$$\eta_{-\mathbf{e}_i}(x + a\mathbf{e}_i) = \eta_{\mathbf{e}_i}(x),$$

$$\hat{W}_M = - \sum_p (\hat{U}_p + \hat{U}_p^\dagger),$$

where  $x$  labels sites,  $\ell \equiv (x, n)$  the spatial links pointing along the spatial unit vector  $n$ ,  $p \equiv (x, n, n')$  the spatial plaquettes;  $\hat{E}_{\ell}$  is the electric field operator, which is diagonal in the P-representation

$$\hat{E}_{\ell}|P\rangle = N_{\ell}(P)|P\rangle, \quad (5)$$

where the eigenvalues  $N_{\ell}(P)$  are the number of times that the link  $\ell$  appears in the set of paths  $P$ ;  $\hat{U}_p = \prod_{\ell \in p} \hat{U}_{\ell}$ . The  $\hat{\Phi}_{\ell}$  are ‘‘displacement’’ operators corresponding to the quantity defined in Eq. (2) for the case of a one-link path, i.e.  $P \equiv \ell$ . The realization of the different Hamiltonian terms in this representation is as follows [9].

First, by Eq. (5) the action of the electric Hamiltonian is given by

$$\hat{W}_E|P\rangle = \sum_{\ell} N_{\ell}^2(P)|P\rangle. \quad (6)$$

The interaction term  $\hat{W}_I$  can be written as

<sup>1</sup>For a more detailed exposition of the P-representation and the realization of the different operators see Ref. [9].

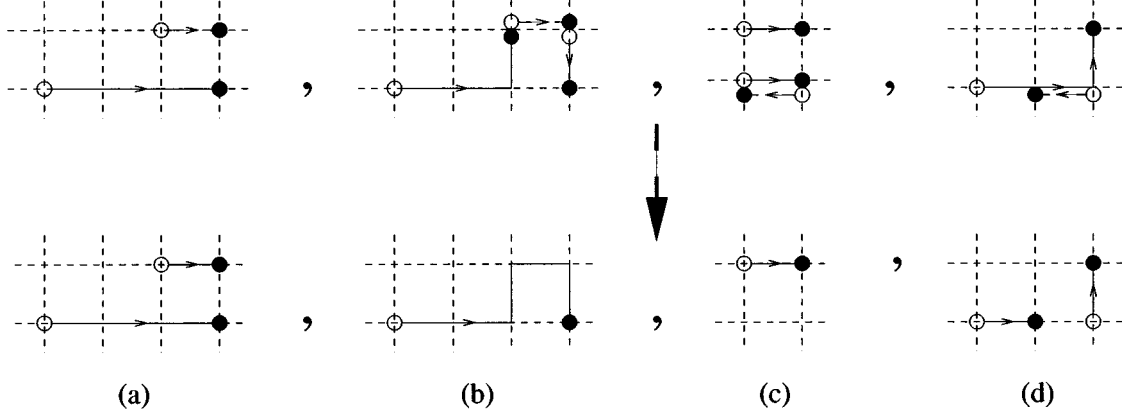


FIG. 1. A summary of the different actions of operators  $\hat{\Phi}_\ell$  applied over path-states  $|P\rangle$ . The link  $\ell$  is represented by a dashed bond in the pictures on the top and the resulting paths  $|P'\rangle$  are plotted below.

$$-\hat{W}_I = \sum_{x_e, n} \hat{\Phi}_n(x_e) + \sum_{x_o, n} \hat{\Phi}_n(x_o),$$

$$\hat{W}_M = \sum_p \eta_p (\hat{U}_p + \hat{U}_p^\dagger),$$

where

where the subscripts  $e$  and  $o$  denote the parity of the lattice sites. This term is realized in  $\{|P\rangle\}$  as

$$\eta_p = \prod_{\ell \in p} \eta_\ell = -1,$$

and then

$$-\hat{W}_I |P\rangle = \sum_{x_e, n} \epsilon(P, \ell_{x_e}) |P \cdot \ell_{x_e}\rangle + \sum_{x_o, n} \epsilon(P, \ell_{x_o}) |P \cdot \ell_{x_o}\rangle \quad (7)$$

$$\hat{W}_M |P\rangle = \sum_p (|P \cdot p\rangle + |P \cdot \bar{p}\rangle) \quad (8)$$

where  $\ell_x$  is the link starting in  $x$  and ending in  $x + na$ . For links of even origin,  $\epsilon(P, \ell)$  is zero whenever an end of  $\ell$  coincides with an end of  $P$ , it is  $-1$  when  $\hat{\Phi}_\ell$  “deletes” the link  $\ell \in P$ , dividing one connected component into two, and it is  $+1$  in any other case. For links of odd origin,  $\epsilon(P, \ell)$  is zero unless both ends of  $\ell$  coincide with two ends in  $P$ . In that case, it is  $-1$  when  $\ell$  joins two disconnected pieces and it is  $+1$  when it closes a connected piece or when it annihilates a link. The different actions of operators  $\hat{\Phi}_\ell$  over path-states  $|P(t)\rangle$  are schematically summarized in Fig. 1.

where  $p$  and  $\bar{p}$  respectively denote the clockwise and the counter-clockwise plaquette contour.

### III. THE WORLD SHEET OR P-ACTION

In order to cast the preceding path description in the Lagrangian formalism let us begin by considering the path integral for lattice QED with staggered fermions. We will show that this leads to a surface action which is not possible to connect directly with the Hamiltonian (4) via the transfer matrix in the Hilbert space  $\{|P\rangle\}$ . However, this action will serve as a guide in order to build the genuine P-action  $S_P$ .

Finally  $\hat{W}_M$  is the sum of the operators  $\hat{U}(p)$  and  $\hat{U}^\dagger(\bar{p})$  which add plaquettes, and can be written as<sup>2</sup>

For simplicity we choose the Villain form of the action, which is given by

$$\begin{aligned} Z &= \int [d\chi^\dagger d\chi] \int [d\theta] \sum_{\{n_p\}} \exp \left\{ -\frac{\beta}{2} \sum_p [\theta_p + 2\pi n_p]^2 + \frac{1}{2} \sum_\ell a^{(D-1)} \eta_\ell (\chi_r^\dagger U_\ell \chi_{r+a\hat{\mu}} + \text{H.c.}) \right\} \\ &= \int [d\chi^\dagger d\chi] \int [d\theta] \sum_n \exp \left\{ -\frac{\beta}{2} \|\nabla \theta + 2\pi n\|^2 + \frac{1}{2} \sum_\ell a^{(D-1)} \eta_\ell (\chi_r^\dagger U_\ell \chi_{r+a\hat{\mu}} + \text{H.c.}) \right\}, \end{aligned} \quad (9)$$

<sup>2</sup>In such a way that a generic path  $P$  is generated out from the 0-path state (strong coupling vacuum) by the application of the operator string  $\hat{\chi}^\dagger(x) \prod_{\ell \in P} \eta_\ell \hat{U}_\ell \hat{\chi}(y)$ .

where we used in the second line the notations of the calculus of differential forms on the lattice of [14]. In the above expression:  $D$  is the lattice dimension,  $\beta=1/e^2$ ,  $\theta$  is a real compact 1-form defined in each link of the lattice,  $U_\ell = e^{i\theta_\ell}$  and  $\chi$  and  $\chi^\dagger$  are Grassmannian variables defined on the sites of the lattice,  $\nabla$  is the co-boundary operator—which maps  $k$ -forms into  $(k+1)$ -forms,  $n$  are integer 2-forms defined at the lattice plaquettes and  $\|g\|^2 = \langle g, g \rangle = \sum_{c_k} g^2(c_k)$ , where  $g$  is any  $k$ -form and  $c_k$  are the  $k$ -cells ( $c_0$  sites,  $c_1$  links,  $\dots$ ). The measure in Eq. (9) is

$$[d\chi^\dagger d\chi] = \prod_r d\chi_r^\dagger d\chi_r, \quad [d\theta] = \prod_\ell \frac{d\theta_\ell}{2\pi}. \quad (10)$$

Let us forget for the moment the global factor  $a^{(D-1)}$ . The equation (9) can be written as

$$\begin{aligned} Z_F &= \int [d\chi^\dagger d\chi] \prod_\ell \exp\{\frac{1}{2} \eta_\ell \chi_r^\dagger U_\ell \chi_{r+a\hat{\mu}}\} \prod_\ell \exp\{\frac{1}{2} \eta_\ell \chi_{r+a\hat{\mu}}^\dagger U_\ell^\dagger \chi_r\} \\ &= \int [d\chi^\dagger d\chi] \prod_\ell (1 + \frac{1}{2} \eta_\ell \chi_r^\dagger U_\ell \chi_{r+a\hat{\mu}}) \prod_\ell (1 + \frac{1}{2} \eta_\ell \chi_{r+a\hat{\mu}}^\dagger U_\ell^\dagger \chi_r); \end{aligned} \quad (13)$$

i.e. in the above product we have to consider each link and its opposite.

Let us recall the rules of Grassmann variables calculus:

$$\{\chi_r, \chi_s\} = \{\chi_r^\dagger, \chi_s^\dagger\} = \{\chi_r, \chi_s^\dagger\} = 0, \quad (14)$$

$$\int d\chi_r = \int d\chi_r^\dagger = 0, \quad (15)$$

$$\int d\chi_r \chi_r = \int d\chi_r^\dagger \chi_r^\dagger = 1. \quad (16)$$

Therefore, when we expand the products in Eq. (13) and the Grassmann variables are integrated out, the only non-vanishing contributions arise from these terms with  $\chi_r^\dagger$  and  $\chi_r$  appearing one and only one time for every site  $r$ . In other words, the integration of the Grassmann variables produce products of  $U_\ell$ 's along closed paths, i.e. Wilson loops. We denote by  $\mathcal{F}$  a generic configuration of multicomponent paths.  $\mathcal{F}$  is specified by a set of oriented links verifying the rule that they enter and leave one and only one time each lattice site  $r$ . This self-avoiding character is the geometric expression of the Pauli exclusion principle.

We distinguish two parts in  $\mathcal{F}$ : the set of connected closed paths where a link is never run in more than once,  $\mathcal{F}^c$  and the set of isolated links traversed in both opposite directions or ‘null’ links  $\tilde{\mathcal{F}}$ . Then  $\mathcal{F} = \mathcal{F}^c \cup \tilde{\mathcal{F}}$ . The number of connected closed components of each kind is called  $N_{\mathcal{F}^c}$  and  $N_{\tilde{\mathcal{F}}}$ . In Fig. 2 we show a two-dimensional sketch on a  $2 \times 2 \times 3$  lattice of a possible configuration  $\mathcal{F}$  consisting in one fermionic loop and two ‘null’ links.

$$Z = \int [d\theta] \exp\{-S_{gauge}(\theta)\} Z_F(\theta), \quad (11)$$

where

$$Z_F = \int [d\chi^\dagger d\chi] \exp\left\{\frac{1}{2} \sum_\ell \eta_\ell (\chi_r^\dagger U_\ell \chi_{r+a\hat{\mu}} + \text{H.c.})\right\}, \quad (12)$$

where  $S_{gauge}$  stands for the pure gauge part and  $Z_F$  denotes the fermionic partition function. Now if we expand the exponential in  $Z_F$  we get

The Grassmann integration over each element of  $\mathcal{F}^c$  or  $\tilde{\mathcal{F}}$  gives a  $-1$ . Thus, after integrating the fermion fields, the fermionic path integral becomes

$$Z_F = \sum_{\mathcal{F}} (-1)^{N_{\mathcal{F}^c}} (-1)^{N_{\tilde{\mathcal{F}}}} \prod_{\ell \in \mathcal{F}^c} \eta_\ell U_\ell, \quad (17)$$

where  $V$  is the total number of lattice sites and we used that the terms  $\eta_\ell U_\ell$  for  $\ell$  in the part  $\tilde{\mathcal{F}}$  of  $\mathcal{F}$  cancel out. It is easy to check that the number  $N_{\tilde{\mathcal{F}}}$  of ‘null’ links in a given  $\mathcal{F}$  is connected with the number  $N_{\mathcal{F}^c}$  of fermionic loops as follows<sup>3</sup>

$$N_{\tilde{\mathcal{F}}} = \frac{V - L_{\mathcal{F}^c}}{2}, \quad (18)$$

where  $L_{\mathcal{F}^c}$  is the number of links in  $\mathcal{F}^c$  (the length). Thus, up to a global sign, we have

$$(-1)^{N_{\tilde{\mathcal{F}}}} = (-1)^{-L_{\mathcal{F}^c}/2}. \quad (19)$$

One can define the  $\eta_{\mathcal{F}^c}$  for a fermionic loop  $\mathcal{F}^c$ :

$$\eta_{\mathcal{F}^c} = \prod_{\ell \in \mathcal{F}^c} \eta_\ell = \prod_{p \in S_{\mathcal{F}^c}} \eta_p = (-1)^{A_{\mathcal{F}^c}}, \quad (20)$$

where  $A_{\mathcal{F}^c}$  is the number of plaquettes which make up any surface  $S_{\mathcal{F}^c}$  enclosed by  $\mathcal{F}^c$  (different choices of  $S_{\mathcal{F}^c}$  dif-

<sup>3</sup>This is true for a lattice with an even number of sites (a lattice with an odd number of sites cannot be ‘filled’ with  $\mathcal{F}$  paths).

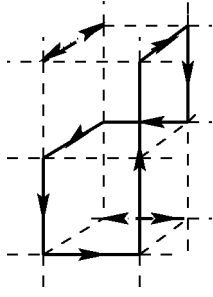


FIG. 2. A possible configuration of self-avoiding paths in a  $2 \times 2 \times 3$  lattice. Fermionic loops are represented by filled bold lines and “null” links by dashed bold lines.

fer by an even number of plaquettes so the sign is well defined and one can choose the  $A_{\mathcal{F}^c}$  as the minimal area bounded by  $\mathcal{F}^c$ ). Neglecting a global sign we get

$$Z_F = \sum_{\mathcal{F}} \sigma_{\mathcal{F}} \prod_{l \in \mathcal{F}^c} U_l, \quad (21)$$

where

$$\sigma_{\mathcal{F}} = (-1)^{N_{\mathcal{F}^c} - L_{\mathcal{F}^c}/2 + A_{\mathcal{F}^c}}. \quad (22)$$

Let us analyze a little closer the sign  $\sigma_{\mathcal{F}}$ . For  $D=2$  we show in Appendix A that all the non-vanishing contributions have  $\sigma_{\mathcal{F}} = +1$ . In more than two space-time dimensions there are non-null contributions  $\mathcal{F}$  to  $Z_F$  with both signs. The reason is that connected fermionic loops enclosing odd numbers of vertices do not necessarily imply any more a null contribution. Different examples of a simple fermionic loop contributing with a  $-1$  are shown in Fig. 3. For instance, in case (a) the enclosed area  $A_{\mathcal{F}^c}$  is 4, the length  $L_{\mathcal{F}^c}$  is 8. Therefore, the fermionic loop (a) has  $N_{\mathcal{F}^c} - L_{\mathcal{F}^c}/2 + A_{\mathcal{F}^c} = 1 - 4 + 4 = 1$ , and then  $\sigma_{\mathcal{F}} = -1$ .

Coming back to the total path integral (9) we can write it as

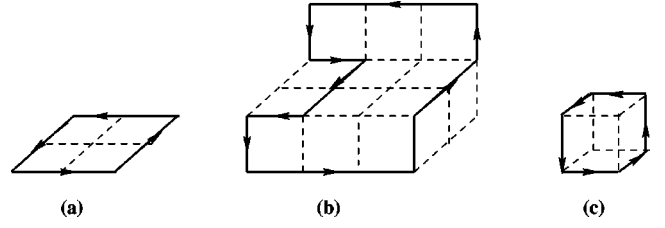


FIG. 3. Different examples of fermionic loops contributing with a  $-1$ .

$$Z = \int [d\theta] \sum_n \sum_{\mathcal{F}} \sigma_{\mathcal{F}}^c \left( \prod_{\ell \in \mathcal{F}^c} U_{\ell} \right) \exp \left\{ -\frac{\beta}{2} \|\nabla \theta + 2\pi n\|^2 \right\}. \quad (23)$$

We can express the fermionic paths  $\mathcal{F}^c$  in terms of integer 1-forms—attached to the links— $f$  with three possible values: 0 and  $\pm 1$  with the constraint that they are non self-crossing and closed  $\partial f = 0$  where  $\partial$  is the boundary operator adjoint of  $\nabla$  which maps  $k$ -forms into  $(k-1)$ -forms. Both operators verify the integration by parts rule

$$\langle \partial g, h \rangle = \langle g, \nabla h \rangle, \quad (24)$$

where  $g$  and  $h$  are respectively  $k$  and  $k-1$  arbitrary forms. The factor  $\prod_{l \in \mathcal{F}^c} U_l$  in Eq. (23) is nothing but the product of Wilson loops along the  $f$ -loops, i.e.  $\exp\{i \sum_{\ell \in \mathcal{F}^c} \theta_{\ell} f_{\ell}\}$ . The  $\tilde{\mathcal{F}}$  can be expressed by means of functions attached to links  $\tilde{f}$  with value 0 or 1 and defined over  $f^{-1}(0)$ , the “nucleus” of  $f$ . In terms of the  $f$  and  $\tilde{f}$  we get

$$Z = \int [d\theta] \sum_n \sum_f \sum_{\tilde{f}} \exp \left\{ -\frac{\beta}{2} \|\nabla \theta + 2\pi n\|^2 + i \langle \theta, f \rangle \right\}. \quad (25)$$

If we use the Poisson summation formula  $\sum_n g(n) = \sum_{n'} \int_{-\infty}^{\infty} dB g(B) e^{2\pi i B n'}$ —where  $n$  and  $n'$  are integer 2-forms and  $B$  is a real 2-form—we get

$$Z = \int [d\theta] \sum_n \sum_f \sum_{\tilde{f}} \sigma(f) \int_{-\infty}^{\infty} [dB] \exp \left\{ -\frac{\beta}{2} \|\nabla \theta + 2\pi B\|^2 + i \langle \theta, f \rangle + 2\pi i \langle B, n \rangle \right\}. \quad (26)$$

Performing the displacement  $B \rightarrow B - \nabla \theta / 2\pi$  and integrating in  $B$ ,

$$\begin{aligned} Z &= \int [d\theta] \sum_n \sum_f \sum_{\tilde{f}} \sigma(f) \exp \left\{ -\frac{1}{2\beta} \|n\|^2 + i \langle \theta, f - \partial n \rangle \right\} \\ &= \sum_n \sum_f \sum_{\tilde{f}} \sigma(f) \exp \left\{ -\frac{1}{2\beta} \|n\|^2 \right\} \delta(f - \partial n) \\ &= \sum_n \sum_f \sigma(\partial n) \exp \left\{ -\frac{1}{2\beta} \|n\|^2 \right\}, \end{aligned} \quad (27)$$

where we have used Eq. (24) in order to transform  $\langle \nabla \theta, n \rangle$  into  $\langle \theta, \partial n \rangle$  whose integration produced the Dirac’s delta

$\delta(f - \partial n)$ . Equation (27) is a geometrical expression of the path integral of lattice QED with staggered fermions in terms of surfaces with self-avoiding boundaries.

Now, let us return to our goal, namely to set up the world sheet Lagrangian formulation corresponding to the P-representation of Sec. II. The path integral (27) includes world sheets of paths with ends of any parity. Therefore, obviously, it does not produce the Hamiltonian (4) by the transfer matrix method.

As a matter of fact, the transfer matrix for staggered fermions is a general and interesting problem on which not much has been done. Unlike the Wilson fermions which come out rather nicely from the transfer matrix [15–17], the staggered fermions present some troubles. For the spatial part of the action the derivation goes in parallel with that for

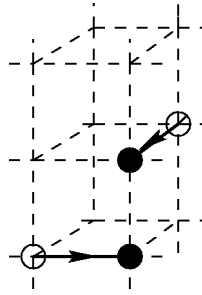


FIG. 4. The P-paths (thick lines) for the different times corresponding to the surfaces enclosed by the configuration of self-avoiding paths of Fig. 2.

the Wilson theory. The interesting question is how does the temporal part work. This problem was discussed in the work of Saratchandra *et al.* [18]; in this paper was analyzed the transfer matrix formalism for relating the Kogut-Susskind Hamiltonian and the Euclidean action for staggered fermion fields. The authors pointed out that the ordinary case, in which the one-component fermions  $\chi(x)$  and  $\chi^\dagger(x)$  both live on all sites, exhibits a doubling of the fermion species with respect to the Hamiltonian formalism (four flavors instead of two flavors). Additionally, the corresponding transfer matrix is Hermitean but not positive definite. They explored the alternative of considering  $\chi$  and  $\chi^\dagger$  on alternate sites; although this procedure avoids the excess of flavors and gives a positive transfer matrix it is not free from complications.

Although the partition function (27) is not directly connected with the Hamiltonian (4) via the transfer matrix, it is closely related with it (as we will show) and provides us with a guide to guess the genuine partition function for the P-representation  $Z_P$ . With this aim we consider the restriction on the set of the surfaces, to the subset of the surfaces such that they are world sheets of the P paths. This is equivalent to require that when intersected with a time  $t = \text{constant}$  plane they give the paths of  $\{P\}$ , i.e. paths with ends of opposite parity and oriented from even sites to odd sites. We get a link of  $P_t$  for every plaquette of the surface which connects the slice  $t$  with the  $t + a_0$ . As an illustration, in Fig. 4 we show the paths of the P-representation we get from the minimal surface enclosed by the configuration of self-avoiding  $\mathcal{F}^c$  paths depicted in Fig. 2.

The imposed constraint forbids fermionic loops such that the one of Fig. 3(c) which gives at the first temporal slice to a path connecting vertices with the same parity. The first configuration with negative Boltzmann factor which appears in the partition function, i.e. that of lower action, is the spatial square of side 2 depicted in Fig. 3(a) with area  $A_{\mathcal{F}^c} = 4$ .

Thus, we propose the following world sheet partition function:

$$Z_P = \sum_S \sigma_h(S) \exp \left\{ -\frac{1}{2\beta_P} \sum_{p \in S} n_p^2 \right\}, \quad (28)$$

where  $S$  runs over world sheets of P-paths and  $\sigma_h(S)$  is a sign defined:

$$\sigma_h(S) = \prod_t (-1)^{A_t} \nu(P_{t-1} \partial S_t) \nu(P_t) \quad (29)$$

where  $S_t$  are the surfaces given by the spatial plaquettes of  $S$  at section  $t$ ,  $A_t$  is the number of plaquettes in  $S_t$  and the function  $\nu$  gives a sign defined by

$$\nu(P) = \prod_\alpha (-1)^{(|P_\alpha| - 1)/2} \prod_\beta (-1)^{|Q_\beta|/2 - 1} \quad (30)$$

( $P = \{P_\alpha, Q_\beta\}$  being  $P_\alpha$  and  $Q_\beta$ , the open and closed component paths respectively. See Appendix B for notation and discussion.) Additionally, note that we have eliminated the sum over the ‘‘null’’ links. The rationale for this is that the ‘‘null’’ links do not play any role in the P-representation. In the next section we are going to show explicitly that  $Z_P$  gives rise to the Hamiltonian (4) via the transfer matrix procedure.

#### IV. HAMILTONIAN OBTAINED VIA THE TRANSFER MATRIX METHOD

By means of the transfer matrix method let us show that we re-obtain the Hamiltonian (4) from the path integral  $Z_P$ . As we wish to consider the continuous time limit of the previous lattice Euclidean space-time theory, we introduce a different lattice spacing  $a_0$  for the time direction. The couplings on timelike and spacelike plaquettes are no longer equal in the action, i.e. we have two coupling constants:  $\beta_0$  and  $\beta_s$ . The temporal coupling constant  $\beta_0$  decreases with  $a_0$  while the spatial coupling constant  $\beta_s$  increases with  $a_0$ . So far we have neglected a factor  $[a^{(D-1)}/2]^V$  in the path integral. Taking into account the fact that the lattice has a different temporal separation  $a_0 \neq a$  we get a relative factor of  $(a_0/a)^{|f|}$  for each spatial link of  $\mathcal{F}^c$ :

$$Z_P = \sum_S a_0^{|\partial n|_{sp}} \sigma_h(S) \exp \left\{ -\frac{1}{2\beta_P} \sum_{p \in S} n_p^2 \right\}, \quad (31)$$

where  $|\partial n|_{sp}$  denotes the number of spatial links in  $\partial n$ . To factorize  $Z_P$  to fixed time contributions we consider the spatial plaquettes of  $S$  that for each  $t$  define the spatial surfaces  $S_t$  and the temporal plaquettes that define the spatial paths  $P_t$  and we write

$$-\frac{1}{2\beta} \|n\|^2 = -\frac{1}{2\beta_s} \sum_t \|n_t\|^2 - \frac{1}{2\beta_0} \sum_t \|P_t\|^2 \quad (32)$$

and

$$\sigma_h(S) = \prod_t \sigma^t(P_{t-1}, P_t, S_t) \quad (33)$$

$$\sigma^t(P_{t-1}, P_t, S_t) = (-1)^{A_t} \nu(P_{t-1} \partial S_t) \nu(P_t). \quad (34)$$

To write the operator  $\hat{T}$  which connects the ket  $|P_{t-1}\rangle$  with the ket  $|P_t\rangle$  we begin by decomposing the sum over world sheets  $\sum_S$  in Eq. (31) into 2 sums: one over the temporal parts, the  $P_t$ , and one over spatial parts  $S_t$ , i.e.

$$Z_P = \sum_{\{P_t\}} \prod_t \langle P_t | \hat{T} | P_{t-1} \rangle$$

$$\langle P' | \hat{T} | P \rangle = \sum_{S_t} a_0^{|\partial S_t|} \bar{p}|_{S_t} \sigma^t \exp \left\{ -\frac{1}{2\beta_0} \|P\|^2 - \frac{1}{2\beta_s} \|n_t\|^2 \right\}. \quad (35)$$

Taking into account the relation which connects  $\hat{T}$  with  $\hat{H}$  when  $a_0$  is small,

$$\hat{T} \propto e^{-a_0 \hat{H} + O(a_0^2)}, \quad (36)$$

we find  $\hat{H}$  considering this limit:

$$\langle P' | \hat{T} | P \rangle \approx \delta_{P',P} - a_0 \langle P' | \hat{H} | P \rangle.$$

The dominant contributions in this limit are the cases where  $P'$  is equal to  $P$  or differs from it by one link  $\ell$  or by one plaquette  $p$ . The power of  $a_0$  in Eqs. (35) forces  $S_t=0$  in the first two cases and  $S_t \equiv p$  in the third:

$$\langle P | \hat{T} | P \rangle \approx 1 \approx \exp \left\{ -\frac{1}{2\beta_0} \|P\|^2 \right\} \quad (37)$$

$$\langle P \cdot p | \hat{T} | P \rangle \approx -a_0 \langle P \cdot p | \hat{H} | P \rangle \approx -\exp \left\{ -\frac{1}{2\beta_s} \right\} \quad (38)$$

$$\langle P \cdot \ell | \hat{T} | P \rangle \approx -a_0 \langle P \cdot \ell | \hat{H} | P \rangle \approx a_0 \sigma^t. \quad (39)$$

To obtain a proper continuum time limit we should take

$$\beta_0 = \frac{a}{g^2 a_0} \quad (40)$$

$$\beta_s = \frac{1}{2} \frac{1}{\ln(2g^2 a/a_0)}, \quad (41)$$

where  $a$  continues to denote the spacelike spacing. The values of  $\sigma^t$  are  $-1$  when adding a plaquette (38) and depend on the way we do it when adding a link (39). An analysis of the possible cases shows that  $\sigma^t$  corresponds to the sign  $\epsilon$  in Eq. (7).

Then,

$$a_0 \hat{H} | P \rangle = \frac{g^2}{2a} \sum_{\mathcal{F}} N_{\mathcal{F}}^2(P) | P \rangle + \frac{1}{2ag^2} \sum_p (|P \cdot p\rangle + |P \cdot \bar{p}\rangle)$$

$$- \frac{1}{2a} \sum_{\mathcal{F}} \epsilon(P, \mathcal{F}) | P \cdot \mathcal{F} \rangle \quad (42)$$

so we recover the Hamiltonian (4), confirming that Eq. (28) is the expression of the partition function of compact electrodynamics in the P-representation.

In Fig. 5 we show a scheme which summarizes the different actions/Hamiltonians for QED with staggered fermions, and their connections. The surface action  $S_{\text{surf}}$  of Eq. (27), which was obtained from the Kogut-Susskind action  $S_{KS}$  by integrating over the gauge and fermion fields, does not produce the Hamiltonian  $H_P$  which in fact is connected

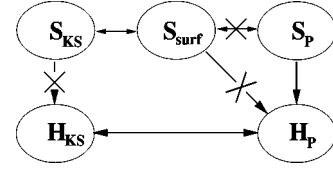


FIG. 5. A diagram summarizing the different lattice actions and Hamiltonians for compact QED and their connections. The horizontal lines denote equivalence. The vertical lines emanating from the classical actions to the Hamiltonians represent the connection via the transfer matrix procedure.

with the  $S_P$  of Eq. (28). This is because  $S_P$  is free from the known problem of  $S_{KS}$  of having an unwanted additional doubling compared with the Hamiltonian formulation. On the other hand, the equivalence between the Kogut-Susskind Hamiltonian  $H_{KS}$  and the P-Hamiltonian  $H_P$  was proved in [9].

In other words, the action  $S_P$  should be regarded as a different lattice action, which produce a Hamiltonian equivalent to the Kogut-Susskind's one.

## V. CONCLUSIONS AND FINAL REMARKS

We propose a purely geometric action in terms of the world sheets of P-path configurations. In this formulation, the connection between the Hamiltonian and Lagrangian of QED with staggered fermions is straightforward via the transfer matrix method. The partition function can be written as a sum over surfaces which border on fermionic self-avoiding loops  $\mathcal{F}^v$ . Hence, the fermionic problem has been reduced to the task of computing quadratic areas enclosed by polymer-like configurations. The polymer representation of lattice fermions [19] is often used in a different way to compute the fermionic determinant. It is important to note that our formalism is free from the problem of the additional doubling of the fermion species due to the discretization of time.

With regard to the economy and possible advantages from the numerical computation point of view offered by the P-description, we want to emphasize two facts: (I) Concerning the gauge degrees of freedom, it only involves sums of gauge invariant variables, i.e. no gauge redundancy. (II) It includes a subset of the configurations which are taken into account in the path integral (27) equivalent to the one of Kogut-Susskind. Our formulation involves a sum of configurations with Boltzmann factors of both signs. However, the lower action configuration with negative Boltzmann factor which appears in the partition function is the spatial square of side 2 which has area  $A_{\mathcal{F}^v} = 4$ . This shows that the positive and negative Boltzmann weights are not balanced and that techniques such as the histogram method [20] can be applied. Equipped with the geometrical insight provided by this gauge invariant representation, we are working to design a suitable algorithm for simulating the loop fermionic action. The simplest case is QED in (1+1) dimensions or the Schwinger model for which all the Boltzmann factors are positive, i.e. one does not have to worry about computing the sign  $\sigma_h(S)$ . In addition, in a two space-time lattice there is a one to one correspondence between fermionic loops and the surfaces with border on them. So, to evaluate the path inte-

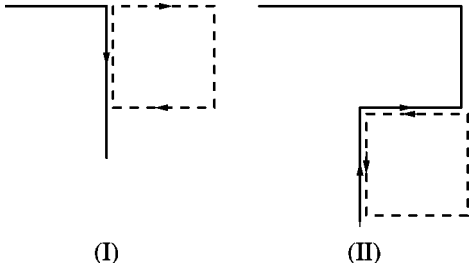


FIG. 6. Two different ways to “append” plaquettes.

gral, the procedure is to generate surfaces with self-avoiding frontiers and with the constraint that they produce on each time slice open paths with ends of opposite parity. This was done recently [21] by means of a Metropolis Monte Carlo algorithm and the results are very encouraging.

Finally, let us mention that in this paper we only considered the simpler Abelian massless theory. In the non-Abelian case (see Ref. [22] for the loop formulation of the pure gauge theory), where there are different colors, the Pauli exclusion principle implies that the maximum number of such pairs at any site cannot exceed the total number of degrees of freedom of the quarks. Therefore, more complicated diagrams arise, for instance, intersecting fermionic loops at vertices where there are more than a  $q\bar{q}$  pair. Here the path to be followed is not unique. It is interesting to consider the massive case too. In this case, in addition to the *dimers*, we would have *monomers* produced by the mass term. The construction of a lattice path integral in terms of loops for *full* QCD is a task that will be considered in a future work.

## ACKNOWLEDGMENTS

We wish to thank helpful comments and remarks from Michael Creutz. This work was supported in part by CONICYT, Projects No. 318 and No. 49.

## APPENDIX A

A general configuration  $\mathcal{F}$  with  $\sigma_{\mathcal{F}} = -1$  obviously must include at least one connected fermionic loop contributing with a  $-1$  to  $\sigma_{\mathcal{F}}$ . We will prove here that such a connected fermionic path necessarily encloses an odd number of sites and thus, in  $D=2$ , it is not possible to “fill” its interior region in such a way that all the sites are “visited” (the condition required for a non-null contribution to  $Z_{\mathcal{F}}$ ).

Notice that, according to Eq. (22), the  $\sigma_{\mathcal{F}}$  associated to a configuration with a unique connected fermionic loop is negative if  $L_{\mathcal{F}^c}/2 + A_{\mathcal{F}^c}$  is an even number.

In order to prove that all the fermionic loops of  $\mathcal{F}^c$  which give a  $-1$  contribution to  $\sigma_{\mathcal{F}}$  enclose an odd number of sites we need to express the number of its inner vertices as a function of its length and area. In  $D=2$ , a generic connected fermionic loop  $\mathcal{F}^c$  enclosing an arbitrary number of vertices can be obtained by a constructive process beginning with a plaquette  $p$  and then generating all the other fermionic loops by “appending” plaquettes to this diagram on each of its links in the two different ways shown in Fig. 6.

The variations of  $N_{\mathcal{F}^c}(L_{\mathcal{F}^c}/2)$  and  $A_{\mathcal{F}^c}$  for the two cases illustrated in Fig. 6 can be summarized as follows:

$$\begin{aligned} \text{(I)} \quad \Delta A_{\mathcal{F}^c} &= 1, \quad \Delta L_{\mathcal{F}^c} = 2, \\ \text{(II)} \quad \Delta A_{\mathcal{F}^c} &= 1, \quad \Delta L_{\mathcal{F}^c} = 0. \end{aligned} \quad (\text{A1})$$

From the above relations it is easy to check

$$\begin{aligned} \Delta A_{\mathcal{F}^c} &= N_{p_I} + N_{p_{II}}, \\ \Delta L_{\mathcal{F}^c} &= 2N_{p_I} \end{aligned} \quad (\text{A2})$$

where  $N_{p_I}$  and  $N_{p_{II}}$  denote the number of plaquettes of type *I* and *II* respectively. It is also easy to see that the number of inner vertices  $I_{\mathcal{F}^c_k}$  to a connected loop is equal to  $N_{p_{II}}$ . Therefore, since  $A_{\mathcal{F}^c} = 1 + \Delta A_{\mathcal{F}^c}$  and  $L_{\mathcal{F}^c} = 4 + \Delta L_{\mathcal{F}^c}$ ,

$$I_{\mathcal{F}^c_k} = 1 - \frac{L_{\mathcal{F}^c}}{2} + A_{\mathcal{F}^c}. \quad (\text{A3})$$

From Eqs. (22) and (A3) we conclude that the contribution of  $\mathcal{F}^c_k$  to  $\sigma_{\mathcal{F}}, \sigma_{\mathcal{F}^c_k}$  is  $-1$  if and only if  $I_{\mathcal{F}^c_k}$  is an odd number.

The same procedure extends to higher dimensions. Equation (A3) is true if the surface is built through steps of type *I*, *II* and *III* where *III* means adding a plaquette making contact in three links of the border. If the surface intersects itself, inner vertices belonging to the intersection lines are counted with the corresponding multiplicity.

## APPENDIX B

### 1. Structure of surfaces

Consider a surface  $S$  contributing to the partition function. Its border is  $C = \partial S$ , a simple loop without intersections (not necessarily connected). This surface carries a sign:

$$\sigma(\partial S) = (-1)^{N-L/2+A} \quad (\text{B1})$$

where

$$N = \text{Number of connected components in } C$$

$$L = \text{Number of links in } C$$

$$A = \text{Number of plaquettes in } S.$$

The sign of  $S$  depends only on  $\partial S$  since two surfaces with the same border differ by an even number of plaquettes.

We divide  $S$  in spatial and temporal plaquettes:  $S = \{S_t, P_t\}$  where

$$S_t = \text{Spatial plaquettes of } S \text{ in the section } t$$

$$P_t = \text{Spatial links in the section } t \text{ corresponding}$$

to temporal plaquettes of  $S$  between  $t$  and  $t+1$ .

Now we have at each spatial section the paths  $\partial S_t$ . Part of these paths propagates to  $t+1$ , part comes from  $t-1$  and part does not propagate and belongs to  $C$ :



$B_t$  = Part of  $\partial S_t$  that does not propagate

$R_t^+$  = Part of  $\partial S_t$  that propagates to  $t+1$

$R_t^-$  = Part of  $\partial S_t$  that comes from  $t-1$

$$\partial S_t = B_t \cdot R_t^+ \cdot R_t^- . \quad (\text{B2})$$

Let us localize now the links of  $C$ . Its temporal links correspond to  $\partial P_t$ . Its spatial links belong to spatial plaquettes, in which case they belong to  $A_t$ , or to temporal plaquettes that can move up or down.

$K_t^+$  = Spatial part of  $C$  in section  $t$  that propagates to

$t+1$

$K_t^-$  = Spatial part of  $C$  in section  $t$  that comes from  $t-1$ .

To keep track of all links in  $S$  (those that belong to any plaquette in  $S$ ) we consider those joining two spatial plaquettes or two temporal plaquettes. The first ones are irrelevant to the sign. The second ones can join two temporal plaquettes in the same section (irrelevant) or in correlative sections:

$\Pi_t$  = Spatial links of  $S$  in section  $t$  that propagate to  $t+1$

and come from  $t-1$ .

To sum up (keys denote the set for all  $t$  and parentheses for a fixed  $t$ )

$$S = \{S_t, P_t\}$$

$$\partial S_t = B_t R_t^+ R_t^-$$

$$C_t = (B_t, K_t^+, K_t^-)$$

$$P_t = (\Pi_t, K_t^+, \bar{R}_t^+)$$

$$C = \{C_t, \partial P_t\}.$$

Note that links in  $B_t, K_t^+, K_t^-$  are incompatible among them while  $\Pi_t, R_t^+, R_t^-$  can share parts among them and with the former.

There is a balance of creation and annihilation

$$\sum_t (|K_t^+| + |R_t^+|) = \sum_t (|K_t^-| + |R_t^-|). \quad (\text{B3})$$

And what leaves at  $t-1$  is what arrives to  $t$ ,

$$P_{t-1} = (\Pi_{t-1}, K_{t-1}^+, \bar{R}_{t-1}^+) = (\Pi_t, \bar{K}_t^-, R_t^-). \quad (\text{B4})$$

It also verifies

$$(-1)^{A-L/2} = (-1) \sum_t A_t^{-1/2} \sum_t (|B_t| + |K_t^+| + |K_t^-|). \quad (\text{B5})$$

## 2. Localization of the sign

The size of an object  $X$  is  $|X|$  = number of links or plaquettes (depending if it is a path or a surface) taking into account its multiplicity. A path is fermionic if it consists of closed single lines and open single lines from even sites to odd sites. For these paths,  $P = \{P_\alpha, Q_\beta\}$  where  $\alpha$  labels the open components and  $\beta$  the closed ones, we define the function

$$\nu(P) = \prod_\alpha (-1)^{|P_\alpha| - 1/2} \prod_\beta (-1)^{|Q_\beta|/2 - 1}. \quad (\text{B6})$$

The meaning of this sign is that it is the sign we get when we create a single line of length  $L$  using only the  $\hat{\Phi}_\ell$  operators. There are  $(L-1)/2$  joining negative actions if the line is open and  $L/2-1$  if the line is closed.

The sign in Eq. (28) is defined

$$\sigma_h(S) = \prod_t (-1)^{A_t} \nu(P_{t-1} \cdot \partial S_t) \nu(P_t) \quad (\text{B7})$$

and it can be written

$$\sigma_h(S) = \prod_t \sigma^t(P_{t-1}, P_t, S_t) \quad (\text{B8})$$

$$\sigma^t(P_{t-1}, P_t, S_t) = (-1)^{A_t} \nu(P_{t-1} \cdot \partial S_t) \nu(P_t). \quad (\text{B9})$$

[1] QCD-TARO Collaboration, in *Lattice '96*, Proceedings of the International Symposium, St. Louis, Missouri, edited by C. Bernard *et al.* [Nucl. Phys. B (Proc. Suppl.) **53**, 938 (1997)]; Philippe de Forcrand, in *Lattice '95*, Proceedings of the International Symposium, Melbourne, Australia, edited by T. D. Kieu *et al.* [*ibid.* **47**, 228 (1996)]; C. Michael, in *Hadron Spectroscopy and the Confinement Problem*, Proceedings, Swansea, Wales, 1995, edited by D. Bugg, NATO Advanced Study Institute Series B: Physics Vol. 353 (Plenum, New York, 1996); G. Lepage and P. Mackenzie, Phys. Rev. D **48**, 2250 (1993).  
[2] R. Gambini and A. Trias, Phys. Rev. D **22**, 1380 (1980).  
[3] R. Gambini and A. Trias, Nucl. Phys. **B278**, 436 (1986).

[4] A. M. Polyakov, Phys. Lett. **82B**, 249 (1979); Nucl. Phys. **B164**, 171 (1979).  
[5] Yu. Makeenko and A. A. Migdal, Phys. Lett. **88B**, 135 (1979).  
[6] C. N. Yang, Phys. Rev. Lett. **33**, 445 (1974).  
[7] A. Ashtekar, Phys. Rev. Lett. **57**, 2244 (1986); Phys. Rev. D **36**, 1587 (1987).  
[8] L. Susskind, Phys. Rev. D **16**, 3031 (1977); T. Banks, D. R. T. Jones, J. Kogut, S. Raby, P. N. Scharbach, D. K. Sinclair, and L. Susskind, *ibid.* **15**, 1111 (1977).  
[9] H. Fort and R. Gambini, Phys. Rev. D **44**, 1257 (1991).  
[10] J. M. Aroca and H. Fort, Phys. Lett. B **317**, 604 (1993).  
[11] J. M. Aroca and H. Fort, Phys. Lett. B **332**, 153 (1994).

- [12] J. M. Aroca, M. Baig, and H. Fort, Phys. Lett. B **336**, 54 (1994).
- [13] J. M. Aroca, M. Baig, H. Fort, and R. Siri, Phys. Lett. B **366**, 416 (1995).
- [14] A. H. Guth, Phys. Rev. D **21**, 2291 (1980).
- [15] M. Creutz, Phys. Rev. D **35**, 1460 (1987).
- [16] M. Creutz, Phys. Rev. D **15**, 1128 (1977).
- [17] M. Lüscher, Commun. Math. Phys. **54**, 283 (1977).
- [18] H. S. Sharatchandra, H. J. Thun, and P. Weisz, Nucl. Phys. **B192**, 205 (1981).
- [19] I. Montvay and G. Münster, *Quantum Fields on the Lattice* (Cambridge University Press, Cambridge, England, 1994).
- [20] A. M. Ferrenberg and R. H. Swendsen, Phys. Rev. Lett. **61**, 2635 (1988).
- [21] H. Fort, Numerical Computations in the Worldsheet Formulation of Lattice Gauge theories, in Lattice '97, Edinburgh, 1997 (in press).
- [22] J. M. Aroca, H. Fort, and R. Gambini, hep-lat/9703007.